



Quasideuteron distribution in nuclei

A. Yu. Illarionov¹

*Dipartimento di Fisica "Enrico Fermi", Università di Pisa,
and INFN, Sezione di Pisa*

REFERENCES:

- O. Benhar, A. Fabrocini, S. Fantoni, A.Yu. I., G.I. Lykasov: **Nucl. Phys. A703**
(2002) 70–82;
O. Benhar, A. Fabrocini, S. Fantoni, A.Yu. I., G.I. Lykasov: **Phys. Rev. C67**
(2003) 014326.

¹on leave of absence from the Joint Institute for Nuclear Research, 141980 Dubna, Moscow region, Russia



- ▶ We compute the distribution of **quasideuterons (QD)** in doubly closed shell nuclei and infinite nuclear matter.
- ▶ The ground states of ^{16}O and ^{40}Ca are described in ls coupling using a realistic hamiltonian including the Argonne v'_8 and the Urbana IX models of two- and three-nucleon potentials, respectively.
- ▶ The nuclear wave function contains central and tensor correlations, and **correlated basis functions theory** is used to evaluate the distribution of neutron-proton pairs, which have the deuteron quantum numbers, as a function of their total momentum.
- ▶ By computing the number of deuteron-like pairs we are able to extract the **Levinger's factor** and compare to both the available experimental data and the predictions of the local density approximation, based on nuclear matter estimates.
- ▶ The **agreement with the experiments is EXCELLENT**, whereas the local density approximation is shown to sizably overestimate the Levinger's factor in the region of the medium nuclei.



Formalism

In a A -nucleon system the distribution of **QD** pairs, whose center of mass is in the orbital state specified by the quantum number X , can be written

$$P_D(X) = \frac{1}{2J_D + 1} \langle A | (a_D^\alpha)^\dagger(X) a_D^\alpha(X) | A \rangle ,$$

where $|A\rangle$ denotes the A -body ground state and $J_D = 1$ is the spin of the deuteron. The operator $a(a^\dagger)_D^\alpha(X)$ annihilates (creates) a deuteron with the quantum number X in the $\alpha = 1, 2, 3$ Cartesian state.

In configuration space the above expression takes the form

$$P_D(X) = \frac{1}{2J_D + 1} \frac{1}{2} \int d^3r_1 d^3r_2 d^3r_{1'} d^3r_{2'} \Psi_{D,cm}(X; \mathbf{R}_{12}) \\ \times \rho_D^{(2)}(\mathbf{r}_1, \mathbf{r}_2; \mathbf{r}_{1'}, \mathbf{r}_{2'}) \Psi_{D,cm}^*(X; \mathbf{R}_{1'2'}) ,$$

where $\rho_D^{(2)}(\mathbf{r}_1, \mathbf{r}_2; \mathbf{r}_{1'}, \mathbf{r}_{2'})$ is a *generalized two-body density matrix* defined by

$$\rho_D^{(2)}(\mathbf{r}_1, \mathbf{r}_2; \mathbf{r}_{1'}, \mathbf{r}_{2'}) = A(A-1) \int d\tilde{R} \Psi_A^*(\mathbf{r}_1, \mathbf{r}_2, \tilde{R}) \psi_{D,rel}^\alpha(12) \\ \times |00\rangle \langle 00| (\psi_{D,rel}^\alpha(1'2'))^* \Psi_A(\mathbf{r}_{1'}, \mathbf{r}_{2'}, \tilde{R}) ,$$

where $|00\rangle$ is the spin-isospin singlet NN state and summation over the repeated indices is understood.



A realistic A -body wave function, accounting for both short- and intermediate-range correlations induced by the strong nuclear interaction, is given in CBF theory by

$$\Psi_A(R) = \mathcal{S} \left[\prod_{i < j} F(ij) \right] \Phi_0(R),$$

where $R \equiv (\mathbf{r}_1, \dots, \mathbf{r}_A)$, \mathcal{S} is a symmetrization operator and Φ_0 is the Slater determinant of single particle orbitals $\phi_\alpha(i)$, which are eigenfunctions of a suitable single particle hamiltonian. For nuclear matter, the orbitals $\phi_\alpha(i)$ are plane waves corresponding to a noninteracting Fermi gas of nucleons with momenta $|\mathbf{k}| \leq k_F = (6\pi^2 \rho_{NM}/\nu)^{1/3}$. $\nu = 4$ and ρ_{NM} are the NM spin-isospin degeneracy and density, respectively.

Pandharipande, Wiringa (1979)

The two-body correlation operator, $F(ij)$, is given by the sum of 6 central and non-central spin-isospin dependent components,

$$\begin{aligned} F(ij) = & f_c(r_{ij}) + f_\sigma(r_{ij})(\boldsymbol{\sigma}_i \cdot \boldsymbol{\sigma}_j) + f_\tau(r_{ij})(\boldsymbol{\tau}_i \cdot \boldsymbol{\tau}_j) \\ & + f_{\sigma\tau}(r_{ij})(\boldsymbol{\sigma}_i \cdot \boldsymbol{\sigma}_j)(\boldsymbol{\tau}_i \cdot \boldsymbol{\tau}_j) + f_t(r_{ij})T_{\alpha\beta}(\hat{\mathbf{r}}_{ij})\sigma_i^\alpha \sigma_j^\beta \\ & + f_{t\tau}(r_{ij})T_{\alpha\beta}(\hat{\mathbf{r}}_{ij})\sigma_i^\alpha \sigma_j^\beta (\boldsymbol{\tau}_i \cdot \boldsymbol{\tau}_j), \end{aligned}$$

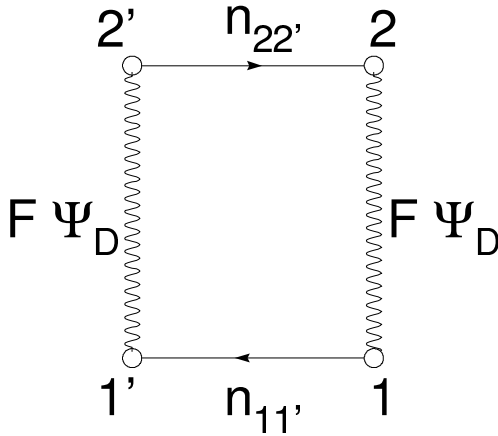
where the $f_p(r)$ correlation functions are variationally fixed by minimizing the ground state energy. All the correlation functions heal to zero, except $f_c(r \rightarrow \infty) \rightarrow 1$, while the tensor operator reads

$$T^{\alpha\beta}(\hat{\mathbf{r}}_{ij}) = 3\hat{r}_{ij}^\alpha \hat{r}_{ij}^\beta - \delta^{\alpha\beta}.$$

A. Fabrocini, A. de Saavedra, and G. Co' (2000)



The dressed leading order approximation



$$\rho_D^{(2)}(\mathbf{r}_1, \mathbf{r}_2; \mathbf{r}_{1'}, \mathbf{r}_{2'}) \approx \frac{2J_D + 1}{4\pi} \rho^{(1)}(\mathbf{r}_1, \mathbf{r}_{1'}) \Sigma(\mathbf{r}_{12}, \mathbf{r}_{1'2'}) \rho^{(1)}(\mathbf{r}_2, \mathbf{r}_{2'}),$$

where $\rho^{(1)}(\mathbf{r}_1, \mathbf{r}_{1'})$ is the one-body density matrix and

$$\Sigma(\mathbf{r}, \mathbf{r}') = \frac{1}{16} [U(r)U(r') + W(r)W(r')Q(\hat{\mathbf{r}} \cdot \hat{\mathbf{r}}')],$$

with $Q(x) = (3x^2 - 1)/2$ and

$$U(r) = u_D(r) - \Delta u(r);$$

$$W(r) = w_D(r) - \Delta w(r).$$

The $\Delta u(r)$ and $\Delta w(r)$ functions account for the medium correlations effect on the bare components of the DWF:

$$\Delta u(r) = u_D(r) [h_c(r) - f_\sigma(r) + 3f_\tau(r) + 3f_{\sigma\tau}(r)] - 2\sqrt{2}w_D(r) [f_t(r) - 3f_{t\tau}(r)];$$

$$\Delta w(r) = w_D(r) [h_c(r) - f_\sigma(r) + 3f_\tau(r) + 3f_{\sigma\tau}(r)] - 2\sqrt{2} \left(u_D(r) - \frac{w_D(r)}{\sqrt{2}} \right) [f_t(r) - 3f_{t\tau}(r)].$$

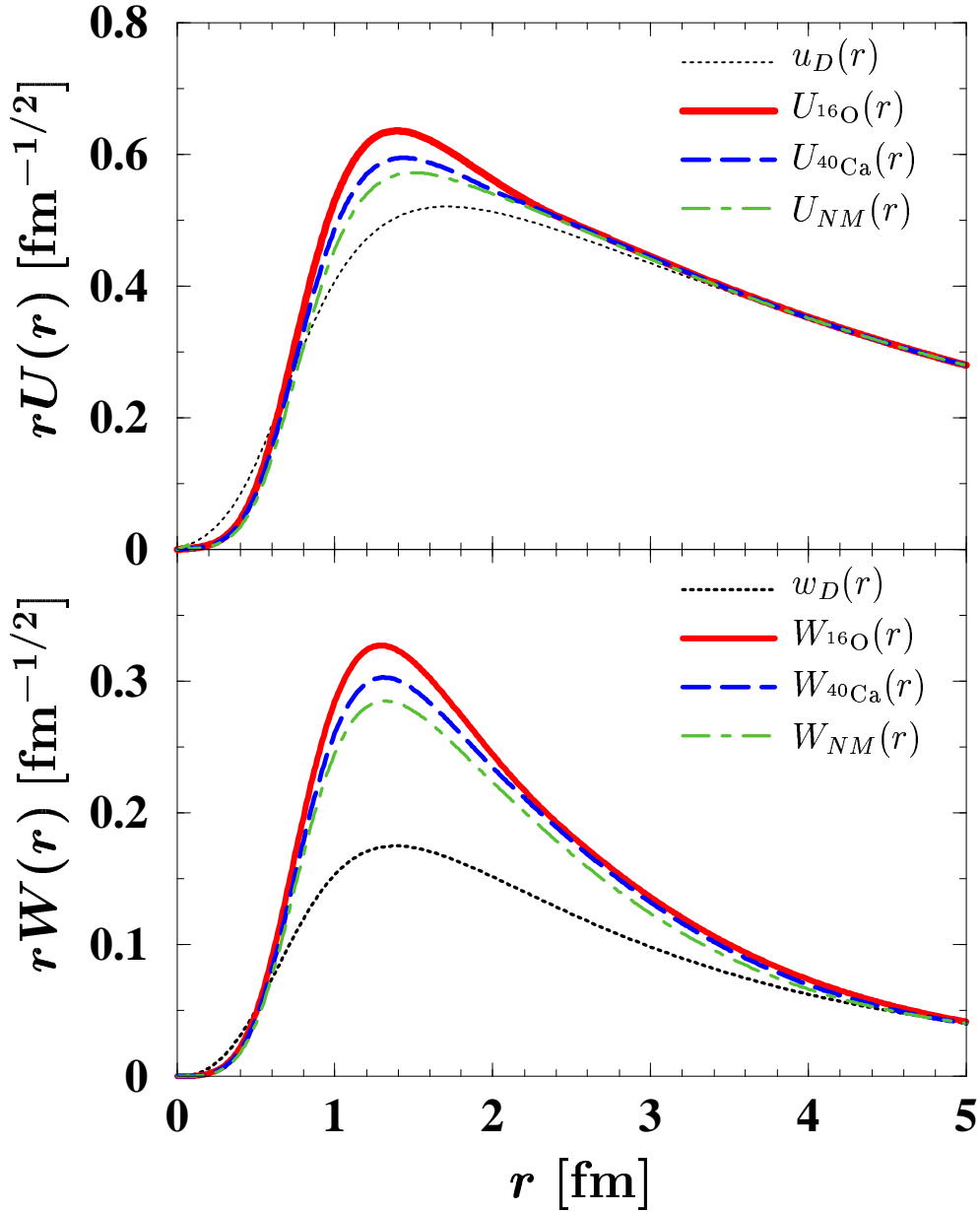
In order to evaluate $\mathcal{P}_D(\mathbf{k}_D)$ in spherically symmetric nuclei, the one-body density matrix can be expressed in terms of the **natural orbits (NO)**:

$$\rho^{(1)}(\mathbf{r}_1, \mathbf{r}_{1'}) = \nu \sum_l \frac{2l+1}{4\pi} P_l(\hat{\mathbf{r}} \cdot \hat{\mathbf{r}}') \sum_n n_{nl} \phi_{nl}^{NO}(r_1) \phi_{nl}^{NO}(r_{1'}).$$

A. Fabrocini, G. Co' (2001)



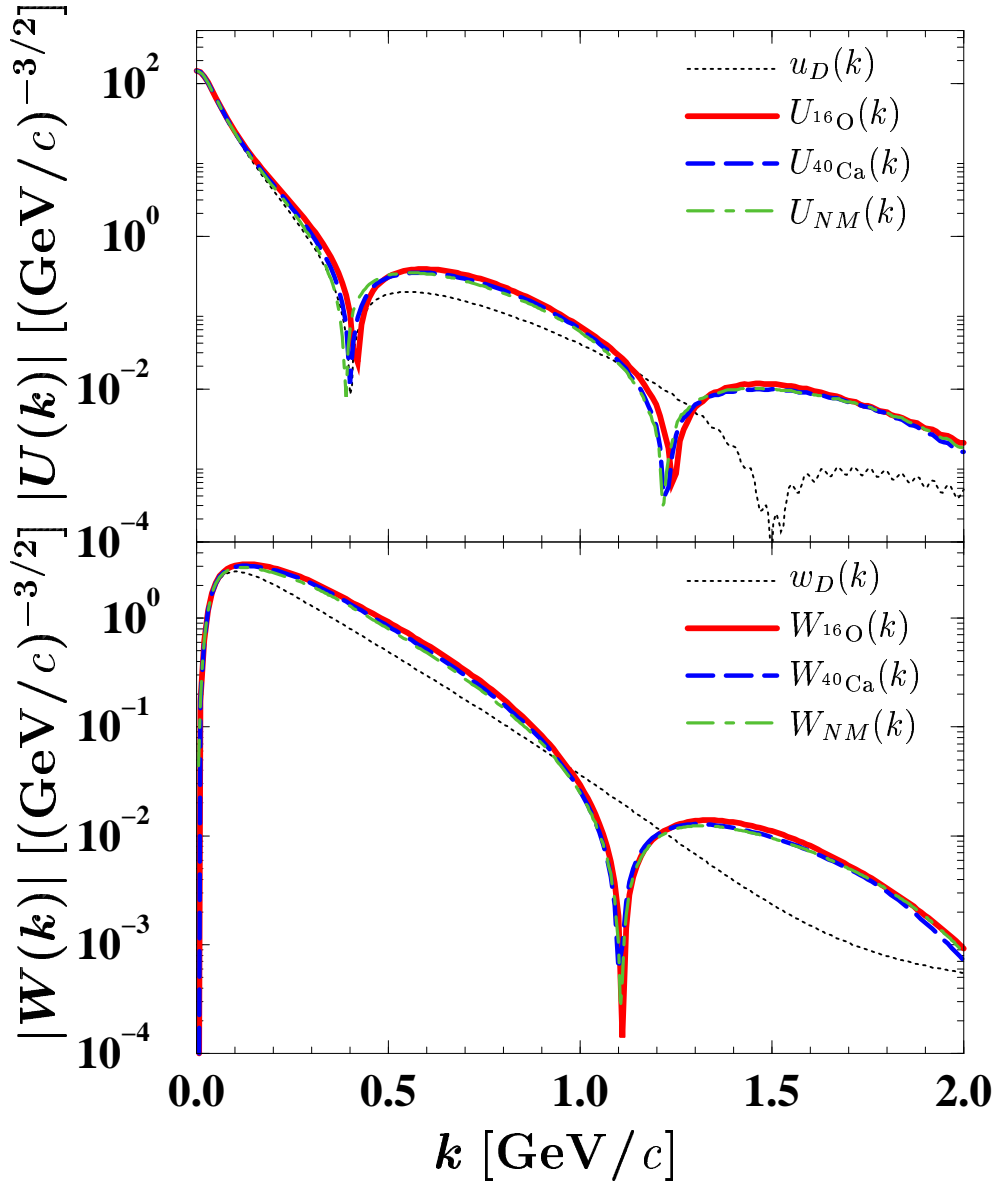
Figure 1: **Radial components $U(r)$ and $W(r)$ of the AU8' QD wave functions** in ^{16}O , ^{40}Ca and **nuclear matter**. **Upper panel:** the solid and dashed lines show the radial dependence of $U_A(r)$ for ^{16}O and ^{40}Ca respectively. The dot-dashed and dotted lines correspond to the nuclear matter $U_{NM}(r)$ and the bare $u_D(r)$. **Lower panel:** as in the upper panel for the D -wave components of the QD and deuteron wave functions.



At small relative distances both $U(r)$ ($r \lesssim 1$ fm) and $W(r)$ ($r \lesssim 0.5$ fm) are slightly suppressed with respect to $u_D(r)$ and $w_D(r)$. On the other hand, they are appreciably enhanced at larger distances. These effects are more visible for the lightest nucleus.



Figure 2: **Radial components $U(k)$ and $W(k)$ in momentum space of the AU8' QD wave functions** in ^{16}O , ^{40}Ca and nuclear matter. **Upper panel:** the solid and dashed lines show the radial dependence of $U_A(r)$ for ^{16}O and ^{40}Ca respectively. The dot-dashed and dotted lines correspond to the nuclear matter $U_{NM}(r)$ and the bare $u_D(r)$. **Lower panel:** as in the upper panel for the D -wave components of the QD and deuteron wave functions.



The nuclear medium shifts the second minimum of $|u_D(k)|$ towards lower values of k . The Argonne v'_8 $|w_D(k)|$ does not exhibit any diffraction minimum, which, however, appears in $|W(k)|$.



QD distribution in a nuclei

$$\mathcal{P}_D(\mathbf{k}_D) = \sum_{\alpha, \alpha'} n_\alpha n_{\alpha'} \mathcal{P}_D^{\alpha, \alpha'}(\mathbf{k}_D),$$

with

$$\mathcal{P}_D^{\alpha, \alpha'}(\mathbf{k}_D) = \frac{\nu^2}{16} \frac{(2\pi)^3}{4\pi} \left[|\Psi_S^{\alpha, \alpha'}(\mathbf{k}_D)|^2 + \sum_{s=-2}^2 |\Psi_D^{\alpha, \alpha'; s}(\mathbf{k}_D)|^2 \right],$$

where $\alpha = (nlm)$,

$$\Psi_S^{\alpha, \alpha'}(\mathbf{k}_D) = \int d^3k \phi_\alpha^{NO\dagger} \left(\frac{\mathbf{k}_D}{2} + \mathbf{k} \right) U(k) \phi_{\alpha'}^{NO} \left(\frac{\mathbf{k}_D}{2} - \mathbf{k} \right),$$

$$\Psi_D^{\alpha, \alpha'; s}(\mathbf{k}_D) = \sqrt{\frac{4\pi}{5}} \int d^3k \phi_\alpha^{NO\dagger} \left(\frac{\mathbf{k}_D}{2} + \mathbf{k} \right) W(k) \phi_{\alpha'}^{NO} \left(\frac{\mathbf{k}_D}{2} - \mathbf{k} \right) Y_{2s}(\hat{\mathbf{k}}),$$

and

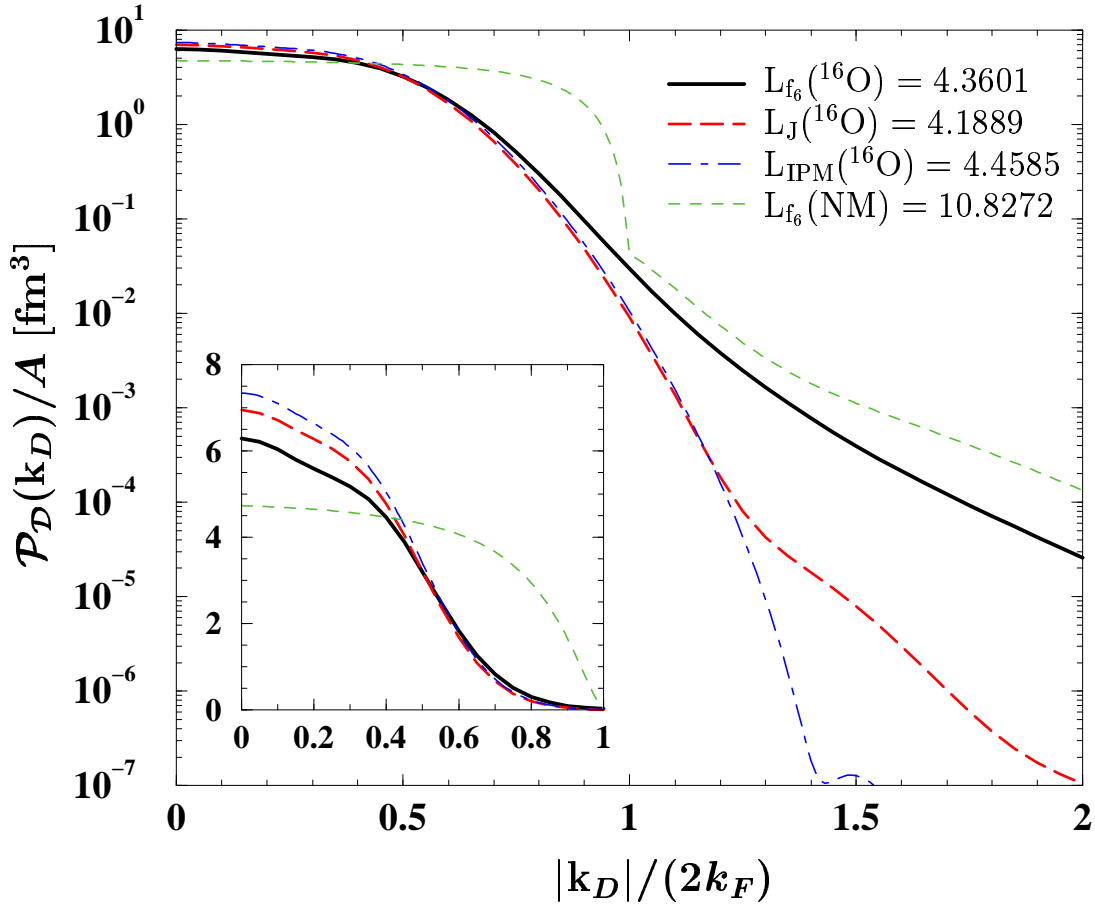
$$\phi_{nlm}^{NO}(\mathbf{q}) = \phi_{nl}^{NO}(q) Y_{lm}(\hat{\mathbf{q}}),$$

$Y_{lm}(\hat{\mathbf{q}})$ are the spherical harmonics.

In the independent particle model (IPM), $\Psi_A(R) \equiv \Phi_0(R)$, and $n_{nl}^{IPM} = 1$, $\phi_{nl}^{NO} \equiv \phi_{nl}$ for occupied states, whereas $n_{nl}^{IPM} = 0$ for unoccupied states. Deviations from IPM provide a measure of correlation effects, as they allow higher NO to become populated with $n_{nl} \neq 0$.



Figure 3: **Momentum distribution of QD pairs in ^{16}O as a function of the total momentum $|\mathbf{k}_D|$.** The solid, dashed and dash-dotted lines are the results obtained within the f_6 and Jastrow correlation models and IPM respectively. The short-dashed line displays the f_6 momentum distribution of the QD in nuclear matter at equilibrium density, $\rho_{NM} = 0.16 \text{ fm}^{-3}$. The insert shows a blow up of the region $|\mathbf{k}_D|/(2k_F) < 1$, plotted in linear scale. The Levinger factors, $L(A)$, for the various calculations are also reported.



- ➔ **NN correlations introduce high momentum components in the distribution.** The full $\mathcal{P}_D(\mathbf{k}_D)$ is strongly enhanced with respect to $\mathcal{P}_D^{IPM}(\mathbf{k}_D)$ at large $|\mathbf{k}_D|$, and it is correspondingly depleted at small $|\mathbf{k}_D|$. The depletion is mostly due to the non-central tensor correlations.
- ➔ **The effect of state-dependent correlations is large**, as one can see by comparing the full $\mathcal{P}_D(\mathbf{k}_D)$ with the Jastrow model $\mathcal{P}_D^J(\mathbf{k}_D)$ (obtained by retaining only the scalar component in the two-body correlation operator).
- ➔ **The tail of $\mathcal{P}_D(\mathbf{k}_D)$ is appreciably different from that of nuclear matter.** At $|\mathbf{k}_D| = 4k_F$ the difference is still a factor ~ 10 for both ^{16}O and ^{40}Ca .



Figure 4: **Momentum distribution of QD pairs in ^{40}Ca as a function of the total momentum $|\mathbf{k}_D|$.** The solid, dashed and dash-dotted lines are the results obtained within the f_6 and Jastrow correlation models and IPM respectively. The short-dashed line displays the f_6 momentum distribution of the QD in nuclear matter at equilibrium density, $\rho_{NM} = 0.16 \text{ fm}^{-3}$. The insert shows a blow up of the region $|\mathbf{k}_D|/(2k_F) < 1$, plotted in linear scale. The Levinger factors, $L(A)$, for the various calculations are also reported.

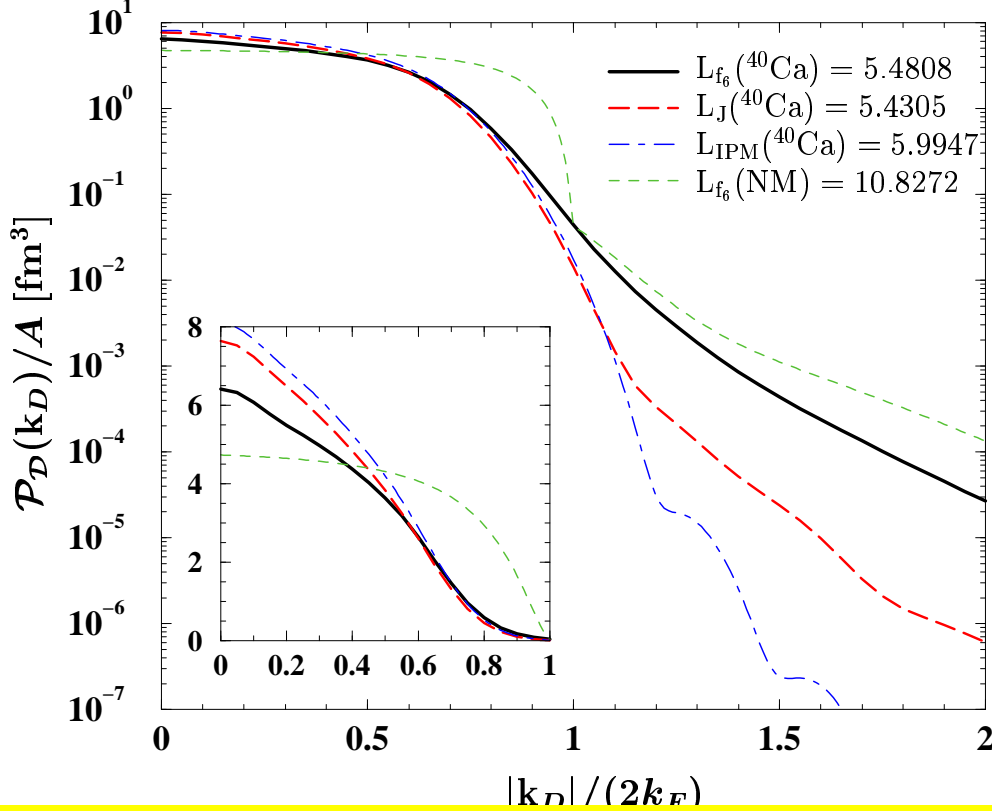
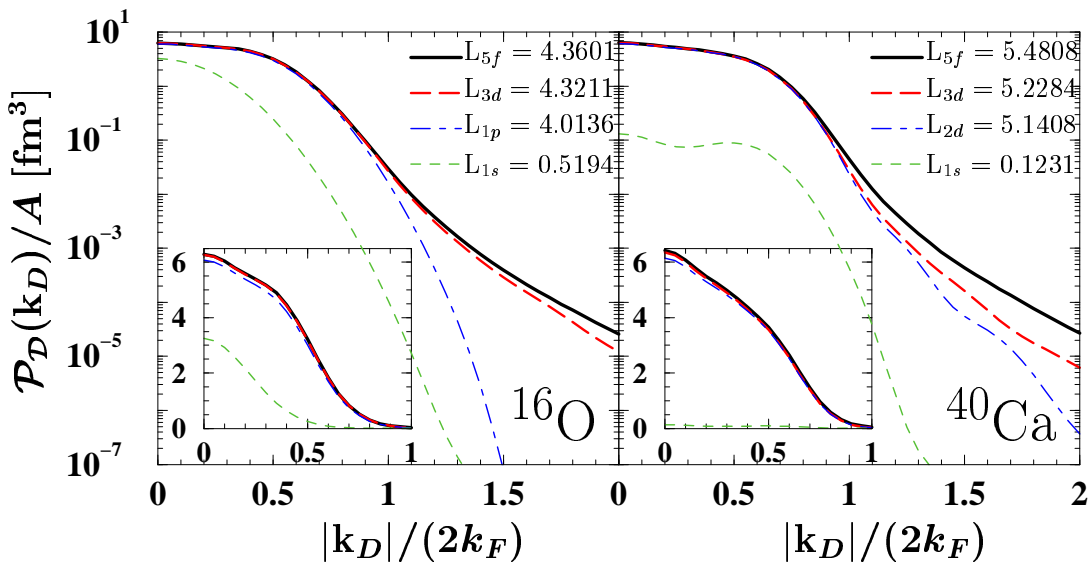


Figure 5: **Convergence of $\mathcal{P}_D(\mathbf{k}_D)/A$ for ^{16}O and ^{40}Ca in the number of natural orbits.** The results have been obtained within the f_6 correlation model.





Levinger's factor

Within the Levinger's **QD** model (1951) the nuclear photoabsorption cross section $\sigma_A(E_\gamma)$, above the giant dipole resonance and below the pion threshold, is

$$\sigma_A(E_\gamma) = \mathcal{P}_D \sigma_{QD}(E_\gamma) ,$$

where E_γ is the photon energy and \mathcal{P}_D is interpreted as the effective number of the NN pairs of the QD type

$$\mathcal{P}_D = \mathbf{L}(A) \left[\frac{Z(A-Z)}{A} \right] ,$$

where $L(A)$ is the so called Levinger's factor.

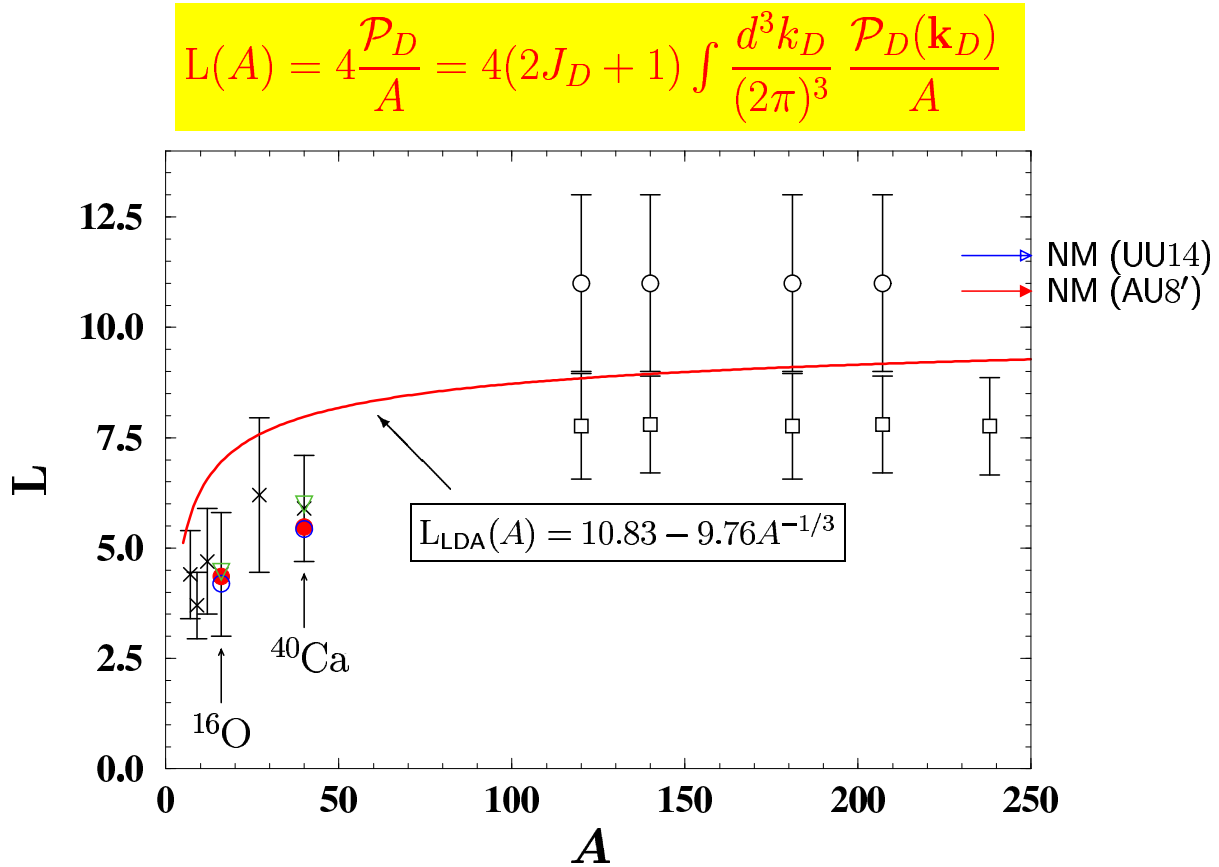


Figure 6: **Levinger's factor** $L(A)$ for ^{16}O , ^{40}Ca and nuclear matter (shown by the arrows for the UU14 and AU8' forces). The filled circles, the empty circles and the triangles show the Levinger's factors obtained within the f_6 and Jastrow correlation models and the IPM, respectively. The LDA is also reported (solid line).



Conclusion

- ★ **CBF** theory has been applied to microscopically compute the distribution of QD pairs, $\mathcal{P}_D(\mathbf{k}_D)$, in doubly closed shell nuclei ^{16}O and ^{40}Ca and **nuclear matter**, starting from the realistic Argonne v'_8 plus Urbana IX potential.
- ★ NN correlations produce a high momentum tail in $\mathcal{P}_D(\mathbf{k}_D)$ and, correspondingly a depletion at small \mathbf{k}_D for both nuclei and nuclear matter. These effects are mainly due to the presence of the state-dependent correlations associated with the tensor component of the one pion exchange interaction. Contrary to what happens for the one-nucleon momentum distribution, this tail sizably differs from that of nuclear matter.
- ★ Summation of $\mathcal{P}_D(\mathbf{k}_D)$ over \mathbf{k}_D provides the total number \mathcal{P}_D of QD pairs and consequently allows for an **ab initio** calculation of the Lvinger's factor $L(A)$. The Lvinger factors for ^{16}O and ^{40}Ca are much smaller than the nuclear matter value and in very good agreement with the available photoreaction data. In addition, our results show that **LDA** overestimates $L(A)$ in the region of the light-medium nuclei.
- ★ The deuteron wave function is appreciably modified by the surrounding medium. While in the case of the S -wave component the difference is mostly visible at small relative distance ($r < 1$ fm), the D -wave component of the **QD** appears to be significantly enhanced, with respect to the deuteron $w_D(r)$, over the range $r < 2$ fm.